

Scintillator Calibration

Latimer D. Harris-Ward
Undergraduate student at the

University of the Pacific, Physics Department

(In collaboration with Kadri B. H. Nizam, Jack Lonergan, Andrew Friedman, and Savio Cao)

(Dated: September 6, 2022)

I. INTRODUCTION

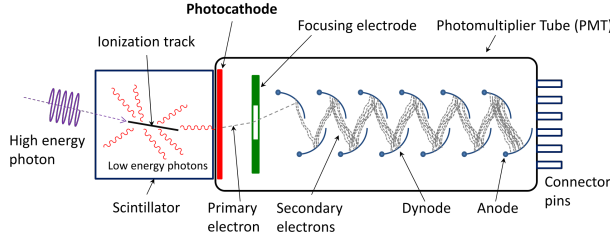


FIG. 1. The different parts of a scintillator.

Purpose

The purposes of this experimentation are as follows: (1) to organize an observation plan with a team, (2) to analyze, understand, and identify various peaks of gamma-ray spectra, and (3) to determine the calibration factor of a Multichannel Analyzer (MCA) using observed channel values and known values for gamma-decay energies. The hypothesis that was considered is “if the channel number is plotted against the gamma-ray energy for various radionuclides, then the observed relationship should be linear.”

The Scintillator

Geiger-Müller (GM) counters are instruments that are good at determining the number of counts detected due to the presence of alpha, beta, and gamma radiation; they are not good at, however, providing information on the energies of the radiation. Scintillators are much better instruments for determining the energies of various gamma ray sources. The reason why scintillators can distinguish between the energies of different gamma ray sources is because of its design. As shown in Figure 1, the scintillator has many components that are essential to its operation. The scintillator is comprised of two primary components: (1) the scintillation chamber and (2) the photomultiplier

tube (PMT). The scintillation chamber consists of a sodium-iodide crystal, sometimes doped with thallium (NaI(Tl)). The PMT contains a photocathode, 10 dynodes, and an anode. In addition to the the scintillation chamber and the PMT, the scintillator counter is connected to a preamplifier and a multichannel analyzer (MCA).

The Production of the Gamma Ray Spectrum

There are various processes that dictate the production of a radionuclide’s gamma ray spectrum. First, the gamma rays emitted by the source enter the scintillation chamber and collide with electrons present in the NaI(Tl) crystal. The underlying processes present when this occurs are Compton Scattering, the photoelectric effect, pair production and annihilation, and/or a combination of the preceding three effects, each with varying energies. Then, the electron passes into the PMT from the scintillation chamber and is directed through the photocathode into a focusing electrode, which sends the primary electron to the first of the ten dynodes. The dynodes serve as electron multipliers and the photocathode coupled with the anode produces a potential difference so as to generate an electric field to carry the multiplied electrons to the anode, where there is an output pulse.

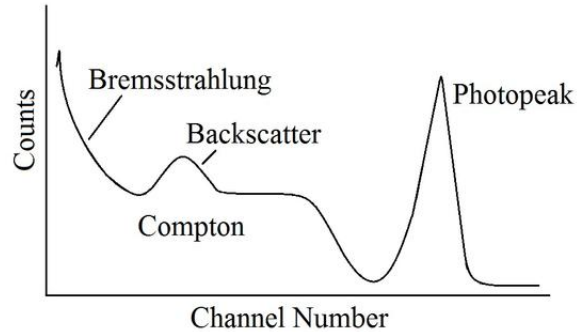


FIG. 2. The various effects present in the scintillation chamber can be seen in the gamma ray spectrum from a monoenergetic γ source.

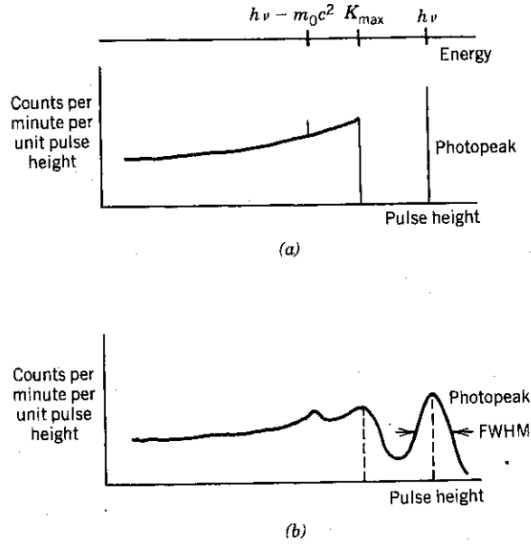


FIG. 3. The difference between an idealized spectrum (a) and an actual spectrum (b).

The time between the initial electron excitation and the output pulse is called the transit time, and it is this time interval that determines the channel and the pulse height of the signal. First, The preamplifier takes weak signal inputs and outputs amplified signals that are strong enough to minimize noise and for further processing, sending them to the MCA. The MCA then takes the input signals and compartmentalizes them into different channels based on the length of the transit time, where the pulse height is proportional to the transit time. Depending on the transit time, this will determine the channel number and the pulse height, both of which produce the overall spectrum, which provides information about the different processes present. As shown in Figure 2, there are several peaks that arise as a consequence of the different processes of the scintillator. The photopeak is produced as a result of the photoelectric effect, where the energy of the gamma ray is completely transferred to the electron in the NaI crystal. The Compton edge, the flat part of the graph, is a consequence of Compton Scattering, where not all of the energy is transferred from the gamma ray to the electron. The backscatter peak results from positron-electron annihilation. Finally, the Bremsstrahlung ("braking radiation") portion of the spectrum arises because of the energies of decelerating electrons scattered by the gamma rays. Figure 3 shows the difference between an idealized gamma ray spectrum and a non-ideal gamma ray spectrum. For the idealized spectrum, the photopeak, the backscattered peak, and the

Compton edge would have infinite resolution. However, due to the fact that other processes are present, affecting the energies of the multiplied electrons in different ways, this causes the resolution to be finite, producing spectra with distributions of counts instead of idealized spectra. As a result, it is important to calibrate scintillators due to the distributive nature of the spectrum. In order to calibrate the scintillator, the spectra of several radionuclides need to be taken, and based on the energies of the radionuclides, a linear relationship is expected, as per the hypothesis presented in the purpose section.

II. DATA ACQUISITION



FIG. 4. The experimental set-up and the elements used to perform the calibration.

Materials

The materials used in the calibration, as per Figure 4, were: the SDA38 NaI(Tl) Detector, the lead shield, the 10 position sample stand, the

BNC connector, the high voltage cable, the USX software, and the gamma ray sources of Na-22, Co-60, and Cs-137, with the Co-60 being the only multi-energetic gamma ray source.

Procedure and Methods

To begin experimentation, the settings of operation were first chosen so as to provide the best resolution of the photopeak. The parameters that were chosen were the coarse gain, the fine gain, the conversion gain, the high voltage, and the preset time. The coarse gain determines how compressed or stretched out the spectrum is. The fine gain and conversion gain together determine the density of channels of the spectrum. The high voltage is used to induce a potential difference to generate an electric field, which carries the multiplied electrons to the anode, and the preset time determines the duration during which the spectrum is obtained. The coarse gain was 16, the fine gain was 1.5, the conversion gain was 1024, the high voltage was 1000 V, and the preset time was 900 seconds, using the real time instead of the live time. The reason for this distinction is because the live time depends on the dead-time and will account for the time during which the scintillator is quenched, not detecting energies. The real time measures the uninterrupted time of measurement. Afterwards, the background spectrum was taken to minimize errors due to counts. Then, the spectra of Na-22, Co-60, and Cs-137 were obtained and analyzed.

III. DATA ANALYSIS

In order to determine the calibration factor of the scintillator counter, the spectra obtained for Na-22, Co-60, and Cs-137 were plotted such that the x-axis was the channel number and the y-axis was the number of counts, with the subtraction of the background from the data set to minimize the error in the number of counts. The channel number is directly proportional to the energy of the electrons detected, depending on which effect was measured by the PMT. Two peaks were fit for both the Na-22 and the Co-60 spectra, whereas one peak was fit for Cs-137 spectrum. The first of the two Na-22 peaks that were fit was the positron-electron annihilation and the second peak was the photopeak. For Co-60, both peaks that were fit were photopeaks and for Cs-137, only one photopeak was fit to the data. The model used for the fits was the Gaussian distribution, given by

$$y = ae^{-\left(\frac{x-b}{c}\right)^2}, \quad (1)$$

where the parameters a , b , and c were fit to the data. The target parameter, though, was the channel number, denoted by b . Because decay events follow Gaussian distributions and they are random and independent, 1000 Monte Carlo fits were performed in order to obtain the channel number for each peak. The fits were performed such that the parameters were chosen so as to minimize the error between the fits and the data. Afterwards, the arithmetic mean was and the standard deviation of the fitted parameters for the channel number were taken to obtain the best approximation of the channel number and the associated uncertainty. Then, the respective fits were superposed onto their original graphs. Afterwards, using the determined channel numbers, the associated uncertainty, and the known energies of the associated peaks, obtained from <http://www.nndc.bnl.gov/nndc/nudat> and www.spectrumtechniques.com/products/sources, a plot of channel number (y-axis) versus energy (x-axis) in megaelectronvolts (MeV) was constructed so as to use linear regression to obtain the parameters for the best fit line. Again, Monte Carlo simulations were used, but 10,000 runs were used for this fit, due to the small uncertainty obtained in the channel number. The errors were assumed to be Gaussian, which allowed for the use of Monte Carlo analysis. Then, the arithmetic mean and the standard deviation of both the fitted slopes and y-intercepts were calculated to obtain the best approximation of the slope and y-intercept of the calibration factor. Lastly, the R^2 value was

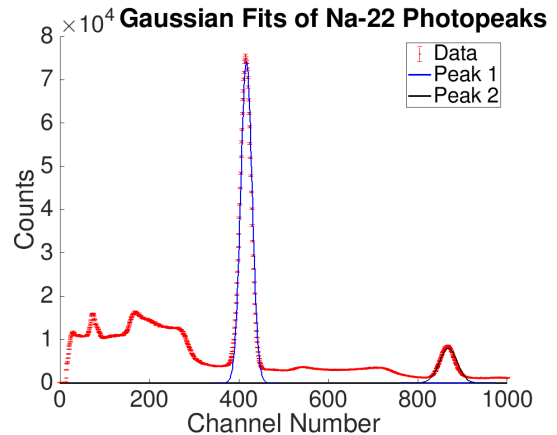


FIG. 5. The Gaussian fits for the annihilation peak and the photopeak of Na-22.

calculated to determine the goodness of the fit.

IV. DISCUSSION

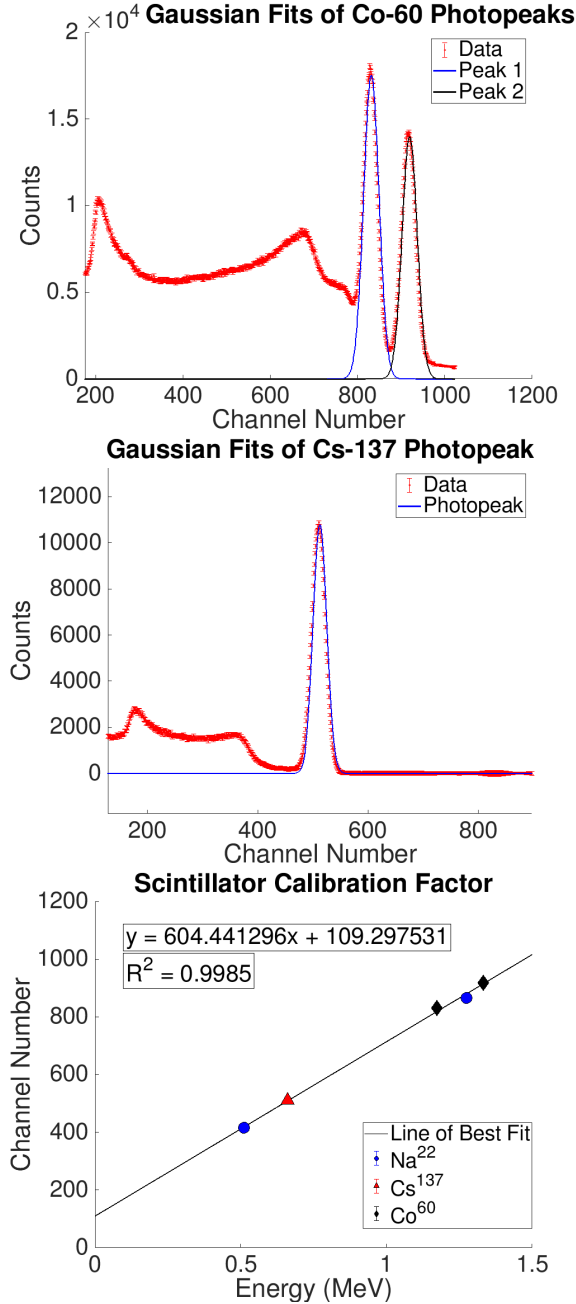


FIG. 6. (Top) The Gaussian fits for the two photopeaks of Co-60. (Middle) The Gaussian fit for the photopeak of Cs-137. (Bottom) The calibration factor of the data.

The values for the measured channel numbers and their associated uncertainties, in the order of Na-22, Co-60, and Cs-137, going from lowest energy to highest energy, are 415.27 ± 0.01 , 866.52 ± 0.04 , 829.76 ± 0.04 , 917.46 ± 0.03 , and 511.23 ± 0.03 , all with the units of channel number. At first glance, it does not make sense for the uncertainty in the channel number to be so small. However, in looking at the data closely, there are many cancellations that occur within the data set, suggesting variability in the data. Thus, in taking the mean and the standard deviation of the fitted values for the channel number, because there are cancellations, the values that occur at higher counts and the values at lower counts than the mean data set do not have an appreciable effect, due to the cancellations. The percent uncertainties in the channel numbers of the aforementioned order are 0.002%, 0.005%, 0.005%, 0.003%, and 0.006%. The low values for the percent uncertainty further exemplify that the data set obtained was distributed uniformly and that the data that was obtained and the fits were good, as seen in Figures 5 and 6. For the linear plot of the channel number versus the energy in MeV, the value of the equation obtained from the Monte Carlo analysis is $y = 604.44x + 109.30$, where the uncertainty in the slope and the y-intercept are ± 0.04 channel/MeV and ± 0.03 channel, respectively. Further, the R^2 value obtained for the goodness of the fit is 0.9985, suggesting that the fit is adequate and good.

According to the bottom image in Figure 5, the channel number for the photopeak for Na-22 is slightly below the line of best fit. The discrepancy between the measured value of 866.52 and the channel number obtained from the line 879.68 is 13.16 channels, which is 329 times greater than the measured uncertainty for the measured channel number. This would suggest that the second data point for Na-22 is significant and should be discarded. In comparison, the calibration factor in the absence of the second Na-22 point is $y = 614.41x + 103.42$ with the same uncertainties as the previous line. Even still, because the uncertainties for the channels are so small, every point has a significant discrepancy, suggesting every point should be discarded. However, due to the statistical nature, this implies that the line of best fit lies within some multiple of the standard deviation. In this case, the multiple is greater than 50 times the standard deviation, which is a consequence of the small standard deviations. Yet, the standard deviation does not allow for the determination of whether differences are statistically significant or not, since they only provide information about how the values vary. In either case, both fits

produce reasonable estimates for the channel number provided some energy and the same is true for the converse. As long as the uncertainties of all parameters are taken into account, then the use of the best fit line should warrant decent approximations of either the channel number or the energy. Additionally, this means that for the scintillator, the calibration factor is reliable, and can be used in further analyses. An application of using the calibration factor is in the determination of the energy or energies of an unknown gamma ray source. So, if an energy is supplied to the calibration factor, then an output should be returned, with some uncertainty in the channel number for error bars.

In this experimentation, the primary sources of uncertainty were the dead time of the scintillator counter, background radiation, and the natural uncertainty in the activity of the radioisotopes. These uncertainties have a direct effect on the number of counts observed for each channel. The dead time produces uncertainty because when the scintillator counter is quenched, the counter is unable to detect additional pulses; however, this effect was reduced because the real time was used instead of the live time. Of course, this is still an instrumental limitation, which will always be present. The background contributes extra counts to the data but the effects were reduced by subtracting the background from collected data. Lastly, because activities can not be measured precisely, there will always be a natural uncertainty with the activity of a radioisotope, which cannot be minimized.

V. CONCLUSION

To conclude, the values for the measured channel numbers and their associated uncertainties, in the order of Na-22, Co-60, and Cs-137, going from lowest energy to highest energy, were 415.27 ± 0.01 , 866.52 ± 0.04 , 829.76 ± 0.04 , 917.46 ± 0.03 , and 511.23 ± 0.03 , all with the units of channel. The very small errors suggest that the data collected was uniform and adequate. The equation of best fit that was determined is $y = 604.44x + 109.30$, where the uncertainties in the slope and y-intercept were ± 0.04 channel/MeV and ± 0.03 channel, respectively. In excluding the photopeak of Na-22, the equation for the calibration factor is $y = 614.41x + 103.42$ with the same exact uncertainties as the previous line. This was done because there is a discrepancy of 13.16 channels between the fit and the Na-22 photopeak channel. Both lines would be sufficient in the determination of the channel number given an energy or the determination of the energy given a channel number; further, no matter which line is used, the line lies outside of the error bars of the points, so the first equation will be used as the calibration factor.

VI. REFERENCES.

1. <http://www.nndc.bnl.gov/nndc/nudat>
2. www.spectrumtechniques.com/products/sources